# Dalton Transactions

Accepted Manuscript






ROYAL SOCIETY OF CHEMISTRY

www.rsc.org/dalton

Textual and Graphical abstract for:

**Mixed amidophenolate-catecholates of molybdenum(VI)**

Sukesh Shekar and Seth N. Brown*

Changing two catecholate ligands to amidophenolates tempers the Lewis acidity of tris(catecholato)molybdenum(VI), but seven-coordinate structures are still observed in the pyridine adduct or in a mixed catecholate-bridged dimer.

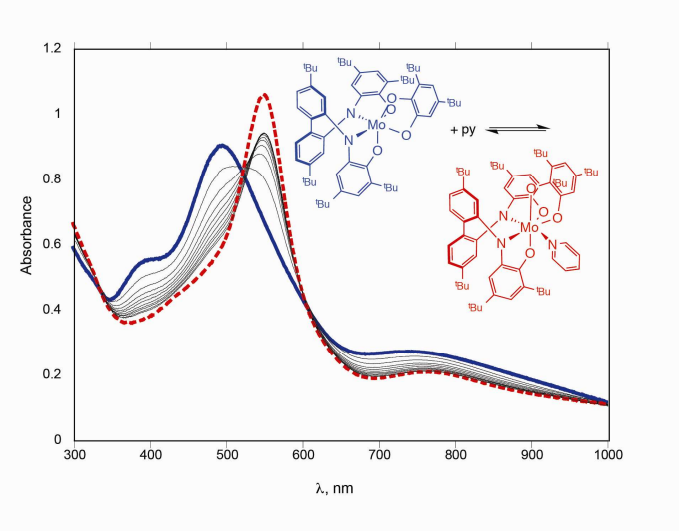

Dalton Transactions

RSCPublishing

ARTICLE

# Mixed amidophenolate-catecholates of molybdenum(VI)

Cite this: DOI: 10.1039/xoxxoooooox

Sukesh Shekar and Seth N. Brown*[a]

Received ooth January 2013,
Accepted ooth January 2013

DOI: 10.1039/xoxxoooooox

www.rsc.org/

The dioxomolybdenum(VI) complex ($^t$BuClipH$_2$)MoO$_2$ ($^t$BuClipH$_4$ = 4,4'-di-*tert*-butyl-*N*,*N*'-bis(3,5-di-*tert*-butyl-2-hydroxyphenyl)-2,2'-diaminobiphenyl) reacts with 3,5-di-*tert*-butylcatechol to form oxo-free ($^t$BuClip)Mo(3,5-$^t$Bu$_2$Cat). The bis(amidophenoxide)-monocatecholate complex is monomeric and exhibits a *cis*-β geometry in the solid state. Variable-temperature NMR data are consistent with two fluxional processes, one that interconverts several geometric isomers at low temperature, and a second that interchanges the ends of the $^t$BuClip ligand at ambient temperatures. The high-temperature fluxional process can be explained by a single Bailar trigonal twist coupled with atropisomerization of the chiral diaminobiaryl backbone. Addition of excess catechol to ($^t$BuClipH$_2$)MoO$_2$ results in formation of a dimolybdenum mono-oxo complex ($^t$BuClip)Mo(μ-3,5-$^t$Bu$_2$Cat)$_2$Mo(O)(3,5-$^t$Bu$_2$Cat). This complex, which contains a seven-coordinate bis(amidophenoxide)molybdenum center and a six-coordinate oxomolybdenum center, represents a structural hybrid between dimeric oxomolybdenumbis(catecholate) and molybdenum tris(catecholate) complexes. Both mono- and dimolybdenum complexes are best formulated as containing Mo(VI), but there is structural evidence for significant π donation from the amidophenolates. ($^t$BuClip)Mo(3,5-$^t$Bu$_2$Cat) binds pyridine to form a mixture of isomeric seven-coordinate adducts. The Lewis acidity of the mixed amidophenoxide-catecholate appears to be lower than its tris(catecholate) or oxobis(amidophenoxide) analogues, which manifests itself principally in relatively slow binding of pyridine to the six-coordinate complex ($k$ = 8 × 10$^4$ L mol$^{-1}$ s$^{-1}$ at 0 ºC) rather than in the rate of dissociation of pyridine from the seven-coordinate adduct.

## Introduction

Catecholates are prototypical redox-active ligands, whose ability to span oxidation states ranging from dianionic to monoanionic (semiquinone) to neutral (quinone) allows them to store redox equivalents. The ability to supply redox equivalents leads not only to a rich coordination chemistry[1] but also to the possibility of performing metal-mediated redox chemistry without requiring an oxidation state change at the metal center.[2] In particular, we recently demonstrated the ability of the oxobis(3,5-di-*tert*-butylcatecholato)molybdenum(VI) moiety to deoxygenate pyridine-*N*-oxide;[3] since the oxygen atom is delivered to Mo but the redox change takes place at the ligands, this oxygen atom transfer reaction can be termed "nonclassical." The tris(catecholato)molybdenum fragment (3,5-$^t$Bu$_2$Cat)$_3$Mo likewise reacts either with dioxygen[4] or pyridine-*N*-oxide[5] to form oxomolybdenum(VI) compounds and 3,5-di-*tert*-butyl-1,2-benzoquinone. These reactions rely on the oxophilicity of Mo(VI) and the reducing power of the catecholates to achieve net oxygen atom transfer.

A serious limitation of the above reactions is the lability of the quinone ligands in their oxidized form. Rapid dissociation of benzoquinone ligands obviates the possibility of catalysis since the oxidized metal complex does not persist long enough to transfer its oxygen atom to a substrate. We were therefore interested in replacing two catecholates with a single, tetradentate bis(amidophenoxide) ligand, since the chelate effect would be expected to stabilize the complex against loss of partially oxidized intermediates. There is precedent for the stability of bis(iminosemiquinonate) complexes of early transition metals.[6] We have previously reported a variety of molybdenum complexes of the 2,2'-biphenyl-bridged bis(amidophenoxide) ligand $^t$BuClip$^{4-}$ ($^t$BuClipH$_4$ = 4,4'-di-*tert*-butyl-*N*,*N*'-bis(3,5-di-*tert*-butyl-2-hydroxyphenyl)-2,2'-diaminobiphenyl) containing ancillary terminal oxo, bridging nitrido, and alkoxide ligands.[7] Here we describe the preparation and characterization of monomeric ($^t$BuClip)Mo(3,5-$^t$Bu$_2$Cat) which contains both catecholate and amidophenoxide ligands. The compound is unsymmetrical in the solid and in solution, but variable-temperature NMR spectra indicate that both geometric isomers and enantiomers interconvert rapidly. We also describe an unsymmetrical dimolybdenum complex, ($^t$BuClip)Mo(μ-(3,5-

$^t$Bu$_2$Cat)$_2$MoO(3,5-$^t$Bu$_2$Cat), which contains both six- and seven-coordinate molybdenum centers.

## Experimental

### General Procedures

Unless otherwise noted, all procedures were carried out under an inert atmosphere in a nitrogen-filled glovebox or on a vacuum line. When dry solvents were needed, chlorinated solvents and acetonitrile were dried over 4 Å molecular sieves, followed by $CaH_2$. Benzene and toluene were dried over sodium, and tetrahydrofuran over sodium benzophenone ketyl. Deuterated solvents were obtained from Cambridge Isotope Laboratories, dried using the same procedures as their protio analogues, and stored in the drybox prior to use. $^t$BuClip$H_4$ (4,4'-Di-*tert*-butylbiphenyl-2,2'-bis((2-hydroxy-3,5-di-*tert*-butylphenyl)amine)), ($^t$BuClip$H_2$)Mo$O_2$, and ($^t$BuClip)Mo(μ-N)(μ-N$H_2$)Mo($^t$BuClip) were prepared as previously described.[7] All other reagents were commercially available and used without further purification. Routine NMR spectra were measured on Varian VXR-300 spectrometer or Bruker Avance DPX 400 spectrometers. Variable-temperature NMR spectra were measured on a Varian Inova 500 spectrometer. Chemical shifts for $^1$H and $^{13}$C{$^1$H} spectra are reported in ppm downfield of TMS, with spectra referenced using the known chemical shifts of the solvent residuals. Infrared spectra were recorded as nujol mulls between NaCl plates on a Jasco 6300 FT-IR spectrometer. ESI mass spectra were obtained using a Bruker micrOTOF-II mass spectrometer, and peaks reported are the mass number of the most intense peak of isotope envelopes. Samples were injected as dichloromethane solutions, preceded and followed by methanol. In all cases, the observed isotope patterns were in good agreement with calculated ones. Elemental analyses were performed by Roberstson Microlit Labs (Ledgewood, NJ) or Midwest Microlab, LLC (Indianapolis, IN).

### Syntheses

**(4,4'-Di-*tert*-butylbiphenyl-2,2'-bis((2-oxy-3,5-di-*tert*-butylphenyl)amido))(3,5-di-*tert*-butylcatecholato)molybdenum(VI), ($^t$BuClip)Mo(3,5-$^t$Bu$_2$Cat).** ($^t$BuClip$H_2$)Mo$O_2$ (0.1544 g, 0.185 mmol) and 3,5-di-*tert*-butylcatechol (3,5-$^t$Bu$_2$Cat$H_2$; Aldrich, 0.0421 g, 0.189 mmol) were weighed in the drybox and dissolved in 4 mL THF. The reaction mixture was stirred for 18 h at room temperature in a sealed reaction vessel. After evaporation of the THF from the dark purple solution *in vacuo*, the crude product was dissolved in 2 mL benzene, filtered through a plug of sand, and layered with 4 mL acetonitrile in a 20 mL scintillation vial. The crystalline product was isolated by filtration, and two subsequent crops were combined to yield 0.1614 g of ($^t$BuClip)Mo(3,5-$^t$Bu$_2$Cat) (85%). $^1$H NMR ($CDCl_3$, 20 ºC, 400 MHz): δ 0.58, 1.15 (s, 9H each, C(C$H_3$)$_3$ from $^t$Bu$_2$Cat), 1.11, 1.19, 1.43 (s, 18H each, C(C$H_3$)$_3$ from $^t$BuClip), 6.29 (d, 2 Hz, 1H, Ar*H* from $^t$Bu$_2$Cat), 6.47 (br s, 2H, Ar*H* from $^t$BuClip), 6.59 (d, 2 Hz, 1H, Ar*H* from $^t$Bu$_2$Cat), 6.81 (d, 2 Hz, 2H, *H*-3), 7.10 (d, 2 Hz, 2H, Ar*H* from $^t$BuClip), 7.22 (dd, 8, 2 Hz, 2H, *H*-5), 7.51 (d, 8 Hz, 2H, *H*-6). $^{13}$C{$^1$H} NMR ($CDCl_3$, 20 ºC, 100.62 MHz): δ 29.69, 29.77, 31.22, 31.75, 31.96 (C(*C*H$_3$)$_3$), 33.95, 34.68, 34.83, 34.98, 35.39 (*C*(CH$_3$)$_3$), 109.30, 110.10, 110.23, 113.41, 121.31, 124.91, 124.93, 125.48, 131.14, 131.51, 134.18, 136.74, 145.03, 146.83, 151.56, 157.10, 158.48, 159.28. IR (cm$^{-1}$): 1601 (w), 1584 (m), 1362 (s), 1307 (m), 1259 (m), 1200 (m), 1169 (s), 1150 (s), 1099 (s), 1026 (m), 992 (s), 944 (m), 912 (m), 853 (m), 762 (m), 721 (w). ESI-MS: 1019.5575 (M+H, calcd 1019.5563). Anal. Calcd for $C_{62}H_{84}MoN_2O_4$ • 1.5 $C_6H_6$: C, 75.17; H, 8.26; N, 2.47. Found: C, 74.83; H, 8.38; N, 2.42.

**(4,4'-Di-tert-butylbiphenyl-2,2'-bis((2-oxy-3,5-di-*tert*-butylphenyl)amido)bis-μ-(3,5-di-*tert*-butylcatecholato)oxo(3,5-di-*tert*-butylcatecholato)dimolybdenum(VI), ($^t$BuClip)Mo(μ-(3,5-$^t$Bu$_2$Cat))$_2$MoO(3,5-$^t$Bu$_2$Cat).** In a 20 mL scintillation vial in the drybox were weighed 0.1772 g $^t$BuClip$H_4$ (0.251 mmol), 0.1639 g dioxomolybdenum bis(acetylacetonate) (Strem, 0.503 mmol, 2.00 equiv), and 0.1672 g 3,5-$^t$Bu$_2$Cat$H_2$ (0.752 mmol, 3.00 equiv). The mixture was dissolved in 5 mL benzene and stirred 48 h. The reaction mixture was filtered through a glass frit and layered with 4 mL dry acetonitrile to yield crystalline product, which was isolated by filtration and washed with 2 × 2 mL acetonitrile. A second crop was isolated from the filtrate on standing to give a total yield of 114.4 mg (29%). $^1$H NMR ($CDCl_3$): δ 0.64, 0.72, 0.79 (s, 9H each, $^t$Bu), 0.93 (s, 18H, 2 × $^t$Bu), 1.01 (s, 27H, 3 × $^t$Bu), 1.15, 1.17, 1.34, 1.43 (s, 9H each, $^t$Bu), 4.79 (d, 2Hz, 1H, Ar*H)*, 5.21 (d, 2 Hz, 1H, Ar*H*), 5.45 (d, 2 Hz, 1H, Ar*H*), 6.37 (d, 2 Hz, 1H, Ar*H*), 6.48 (d, 2 Hz, 1H, *H*-3), 6.55 (m, 3H, *H*-3, 2 × Ar*H*), 6.73 (d, 2 Hz, 1H, Ar*H*), 6.93 (d, 2 Hz, 1H, Ar*H*), 6.98 (d, 2 Hz, 1H, Ar*H*) 7.05 (dd, 8, 2 Hz, 2H, *H*-5), 7.21 (d, 8 Hz, 1H, *H*-6), 7.31 (dd, 8, 2 Hz, 1H, *H*-5), 7.58 (d, 2 Hz, 1H, *H*-6), 7.82 (d, 2 Hz, 1H, Ar*H*). $^{13}$C{$^1$H} NMR ($CDCl_3$): δ 29.93, 29.95, 30.11, 30.17, 30.57, 31.08, 31.31, 31.35, 31.42, 31.65, 32.00, 32.08 (C(*C*H$_3$)$_3$), 34.34, 34.40, 34.56, 34.59, 34.65, 34.74, 34.81, 34.82 (2C), 34.85, 34.88, 35.25 (*C*(CH$_3$)$_3$), 107.53, 107.64, 108.86, 110.56, 115.02, 116.08, 116.52, 118.42, 121.78, 123.41, 123.57, 124.37, 124.99, 125.27, 126.16, 129.96, 130.57, 130.64, 134.33, 135.31, 136.56, 138.26, 138.49, 140.69, 143.44, 143.83, 145.22, 146.90, 148.27, 149.94, 150.01, 151.34, 152.07, 153.08, 153.54, 153.69, 154.65, 155.88, 158.88, 162.60, 163.04, 164.91. IR (cm$^{-1}$): 1583 (m), 1551 (w), 1410 (m), 1387 (m), 1361 (s), 1307 (m), 1253 (m), 1201 (s), 1174 (m), 1149 (w), 1105 (w), 1026 (m), 973 (s), 944 (s), 914 (m), 890 (w), 865 (m), 834 (m), 753 (s), 722 (w), 687 (m), 651 (m), 595 (w), 588 (w). ESI-MS: 1573.7506 (M+H, calcd 1573.7491). Anal. Calcd for $C_{90}H_{124}Mo_2N_2O_9$: C, 68.86; H, 7.96; N, 1.78. Found: C, 68.72; H, 7.67; N, 1.60.

### Variable-temperature NMR spectroscopy

NMR spectra of ($^t$BuClip)Mo(3,5-$^t$Bu$_2$Cat) were recorded between –95 and +21.5 ºC in $CD_2Cl_2$ on a Varian VXR-500 NMR spectrometer. The line shapes of the ligand *tert*-butyl



 

resonances were simulated using the program *g*NMR[8] to generate calculated lineshapes and superimpose them on the observed spectra for temperatures from –30 to +10 ºC.

NMR spectra of ($^t$BuClip)Mo(3,5-$^t$Bu$_2$Cat)(Py), generated *in situ* from ($^t$BuClip)Mo(3,5-$^t$Bu$_2$Cat) and pyridine, were recorded between –40 and +30 °C in $CD_2Cl_2$ on a Varian VXR-500 NMR spectrometer. To determine the rate of dissociation of pyridine at 0º C, the region from δ 7.4-8.6 ppm, containing peaks due to the 2,6- and 4-H signals of bound and free pyridine, were simulated using the program *i*NMR (http://www.inmr.net). In addition to exchange between each of the two sets of bound pyridine signals with free pyridine, a minor amount of direct exchange between the bound pyridine signals was required to achieve a satisfactory fit.

### UV-visible titration of ($^t$BuClip)Mo(3,5-$^t$Bu$_2$Cat) with pyridine

A solution of 2.0 mL of 5 × $10^{-5}$ M ($^t$BuClip)Mo(3,5-$^t$Bu$_2$Cat) in $CH_2Cl_2$ was prepared in the drybox and sealed in a 1-cm quartz screw-cap cuvette using a Teflon-backed silicone rubber septum. Spectra were obtained on a Thermo Scientific Evolution Array UV-Visible spectrophotometer. The cuvette was equilibrated in the instrument's multicell changer, with the temperature controlled by circulation of ethylene glycol/water mixture through the cell holder and measured using a thermocouple inserted in a dummy cuvette. The titration was carried out by sequential injection of aliquots of pyridine dissolved in dichloromethane through the rubber septum of the cuvette.

Binding constants were extracted from simulation of the absorbance data from 300-1000 nm for each titration. The spectrum of ($^t$BuClip)Mo(3,5-$^t$Bu$_2$Cat) was fixed as equal to the initial spectrum in the titration, and the spectrum of the pyridine adduct was removed as an independent parameter using linear least-squares fitting as described in the literature.[9] The binding constant $K_{eq}$ was optimized as the sole adjustable parameter by nonlinear least-squares fitting using the Solver routine in Microsoft Excel.[10] A van't Hoff plot of ln($K_{eq}$) vs. 1/T in the range of 284-308 K was used to calculate thermodynamic parameters for binding.

### DFT Calculations

Geometry optimizations and orbital calculations were performed on all three geometric isomers of ($^t$BuClip)Mo(3,5-$^t$Bu$_2$Cat). The crystal structure of ($^t$BuClip)Mo(3,5-$^t$Bu$_2$Cat) (*vide infra*) was used as the starting geometry in calculations on the *cis*-β1 isomer, and the starting structure of the *cis*-β2 isomer was created by shifting the positions of the *tert*-butyl groups on the 3,5-$^t$Bu$_2$Cat ligand. The crystal structure of ($^t$BuClip)Mo(O$^i$Pr)$_2$[7] was modified to use as a starting structure for the *cis*-α isomer. Calculations used the hybrid B3LYP method, with an SDD basis set for molybdenum and a 6-31G* basis set for all other atoms, using the Gaussian09 suite of programs.[11] The optimized geometries were confirmed as minima by calculation of vibrational frequencies.

### X-ray crystallography

Crystals of ($^t$BuClip)Mo(3,5-$^t$Bu$_2$Cat)•1.5 $C_6H_6$ and ($^t$BuClip)Mo(μ-3,5-$^t$Bu$_2$Cat)$_2$MoO(3,5-$^t$Bu$_2$Cat)•1.5 $C_6H_6$ were grown by layering concentrated solutions in benzene with acetonitrile. Crystals of $Mo_2O_2$(3,5-$^t$Bu$_2$Cat)$_4$•2 $C_6H_6$ formed on attempted recrystallization of ($^t$BuClip)Mo(μ-3,5-$^t$Bu$_2$Cat)$_2$MoO(3,5-$^t$Bu$_2$Cat) from a benzene/acetonitrile mixture that was exposed to air. Crystals were placed in inert oil before transferring to the cold $N_2$ stream of a Bruker Apex II CCD diffractometer. Data were reduced, correcting for absorption, using the program SADABS. The structures were solved using direct methods. All nonhydrogen atoms not apparent from the initial solutions were found on difference Fourier maps, and all heavy atoms were refined anisotropically. The crystal of ($^t$BuClip)Mo(3,5-$^t$Bu$_2$Cat)•1.5 $C_6H_6$ was found to be twinned by examination using the TwinRotMat function in the program PLATON.[12] The twin law was found to be [ -1 0 0 0 -1 0 1 0 1 ], and refinement of the batch structure factor indicated that the extent of twinning was 0.064. Inclusion of this twin law drastically improved the model and eliminated all of the inconsistent equivalents. Two of the *tert*-butyl groups in ($^t$BuClip)Mo(3,5-$^t$Bu$_2$Cat), those bonded to C24 and C45, were disordered in two different orientations, as was the *tert*-butyl group bonded to C18 in $Mo_2O_2$(3,5-$^t$Bu$_2$Cat)$_4$. All nonhydrogen atoms were refined anisotropically. Hydrogen atoms in $Mo_2O_2$(3,5-$^t$Bu$_2$Cat)$_4$•2 $C_6H_6$, except for those on the disordered *tert*-butyl group, were found on difference maps and refined isotropically. All other hydrogen atoms were placed in calculated positions, with thermal parameters for the hydrogens tied to the isotropic thermal parameters of the atoms to which they are bonded (1.5 × for methyl, 1.2 × for all others). Calculations used SHELXTL (Bruker AXS),[13] with scattering factors and anomalous dispersion terms taken from the literature.[14] Further details about the structures are in Table 1.

## Results and Discussion

### Synthesis, structure, and bonding of ($^t$BuClip)Mo(3,5-$^t$Bu$_2$Cat)

The dioxomolybdenum bis(aminophenoxide) complex ($^t$BuClipH$_2$)$MoO_2$ ($^t$BuClipH$_4$ = 4,4'-di-*tert*-butyl-2,2'-bis((2-hydroxy-3,5-di-*tert*-butylphenyl)amino)biphenyl) serves as a useful precursor for other molybdenum complexes containing the $^t$BuClip$^{4-}$ ligand. For example, ($^t$BuClipH$_2$)$MoO_2$ reacts with excess alcohol to form the bis(alkoxide) complexes *cis*-α-($^t$BuClip)Mo(OR)$_2$ (R = $CH_3$, $^i$Pr).[7] In similar fashion, ($^t$BuClipH$_2$)$MoO_2$ reacts with one equivalent of 3,5-di-*tert*-butylcatechol, 3,5-$^t$Bu$_2$CatH$_2$, over the course of a few minutes at room temperature in chloroform or benzene to give ($^t$BuClip)Mo(3,5-$^t$Bu$_2$Cat) as the major product (eq 1). The same product is formed on reaction of 3,5-$^t$Bu$_2$CatH$_2$ with the bridging nitride complex ($^t$BuClip)Mo(μ-N)(μ-$NH_2$)Mo($^t$BuClip). The $^1$H NMR spectrum of the product establishes a 1:1 ratio of $^t$BuClip:$^t$Bu$_2$Cat in the product. Confirmation of the monomeric nature of the complex is provided by observation of the parent ion in the electrospray

**Table 1.** X-ray crystallographic details for ($^t$BuClip)Mo(3,5-$^t$Bu$_2$Cat)•1.5 C$_6$H$_6$, ($^t$BuClip)Mo(μ-(3,5-$^t$Bu$_2$Cat)$_2$)MoO(3,5-$^t$Bu$_2$Cat)•1.5 C$_6$H$_6$, and Mo$_2$O$_2$(3,5-$^t$Bu$_2$Cat)$_4$•2 C$_6$H$_6$.

| | ($^t$BuClip)Mo(3,5-$^t$Bu$_2$Cat)•1.5 C$_6$H$_6$ | ($^t$BuClip)Mo(μ-(3,5-$^t$Bu$_2$Cat)$_2$)MoO(3,5-$^t$Bu$_2$Cat) • 1.5 C$_6$H$_6$ | Mo$_2$O$_2$(3,5-$^t$Bu$_2$Cat)$_4$•2 C$_6$H$_6$ |
|---|---|---|---|
| Molecular formula | $C_{71}H_{93}MoN_2O_4$ | $C_{99}H_{134}Mo_2N_2O_9$ | $C_{68}H_{92}Mo_2O_{10}$ |
| Formula weight | 1134.47 | 1688.05 | 1261.30 |
| *T*/K | 100(2) | 120(2) | 119(2) |
| Crystal system | Monoclinic | Triclinic | Monoclinic |
| Space group | $P2_1/c$ | $P\bar{1}$ | $P2_1/c$ |
| λ/Å | 1.54178 (Cu Kα) | 0.71073 (Mo Kα) | 0.71073 (Mo Kα) |
| Total data collected | 53342 | 53565 | 37715 |
| No. of indep reflns. | 11671 | 18537 | 7332 |
| $R_{int}$ | 0.0497 | 0.0934 | 0.0211 |
| Obsd refls [I>2σ(I)] | 10611 | 11227 | 6694 |
| *a*/Å | 9.6883(2) | 14.429(3) | 11.7617(3) |
| *b*/Å | 24.4093(5) | 14.825(3) | 16.6561(4) |
| *c*/Å | 27.7995(6) | 25.227(3) | 16.5304(4) |
| α/° | 90 | 90.224(5) | 90 |
| β/° | 100.0270(10) | 103.562(5) | 90.3779(11) |
| γ/° | 90 | 118.130(5) | 90 |
| V/Å$^3$ | 6473.7(2) | 4584.8(16) | 3238.30(14) |
| *Z* | 4 | 2 | 2 |
| μ/mm$^{-1}$ | 2.015 | 0.329 | 0.442 |
| Crystal size/mm | 0.78 × 0.76 × 0.11 | 0.19 × 0.08 × 0.06 | 0.53 × 0.51 × 0.17 |
| No. refined params | 724 | 1009 | 519 |
| *R*1, *wR*2 [I > 2σ(I)] | *R*1 = 0.0389, *wR*2 = 0.0958 | *R*1 = 0.0543, *wR*2 = 0.0973 | *R*1 = 0.0222, *wR*2 = 0.0561 |
| *R*1, *wR*2 [all data] | *R*1 = 0.0450, *wR*2 = 0.1000 | *R*1 = 0.1146, *wR*2 = 0.1176 | *R*1 = 0.0252, *wR*2 = 0.0581 |
| Goodness of fit | 1.030 | 0.969 | 1.029 |

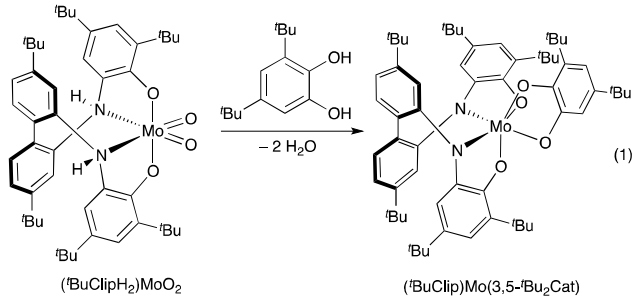


($^t$BuClipH$_2$)MoO$_2$ ($^t$BuClip)Mo(3,5-$^t$Bu$_2$Cat)

mass spectrum and by the solid-state structure determined by X-ray crystallography (Figure 1).

The solid-state structure of ($^t$BuClip)Mo(3,5-$^t$Bu$_2$Cat) is roughly octahedral, with some distortion toward a trigonal prismatic geometry, as previously observed for six-coordinate complexes of the $^t$BuClip ligand[7] and the analogous bis(amidophenoxide) ligand bridged by an unsubstituted 2,2'-biphenyl linker.[15] The monomeric nature of the structure is noteworthy, as isoelectronic (3,5-$^t$Bu$_2$Cat)$_3$Mo forms a seven-coordinate dimer in the solid state.[5] While the $^t$BuClip ligand is not well-suited to bridging because of the *tert*-butyl groups *ortho* to the aryloxides, the catecholate should be able to bridge, as in Mo$_2$(3,5-$^t$Bu$_2$Cat)$_6$. The monomeric structure is thus an electronic consequence of enhanced donation from the amidophenoxide ligands compared to catecholate. The bis(amidophenoxide) ligand is sterically constrained to adopt a *cis* configuration, and in this complex it adopts a structure where the aryloxide oxygen O2 is *trans* to one of the amido nitrogen atoms (N1), the so-called *cis*-β isomer,[16] though *cis*-α

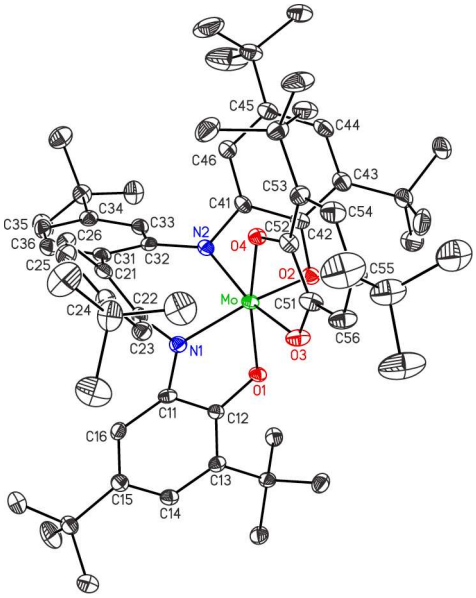


Figure 1. Thermal ellipsoid plot of ($^t$BuClip)Mo(3,5-$^t$Bu$_2$Cat)•1.5 C$_6$H$_6$, with hydrogen atoms and lattice solvent omitted for clarity. Only the major orientation of the *tert*-butyl groups bonded to C24 and C45 are shown.

compounds (with the aryloxide oxygens mutually *trans*) can also be formed by this ligand.

All bond lengths to molybdenum are similar (Table 2), with Mo–O and Mo–N distances between 1.95–2.03 Å. The greatest asymmetry is in the binding of the 3,5-$^t$Bu$_2$Cat ligand, with O3 forming the longest bond to molybdenum (2.0288(18) Å) and

**Table 2.** Selected bond distances (Å) and angles (deg) in ($^t$BuClip)Mo(3,5-$^t$Bu$_2$Cat)•1.5 C$_6$H$_6$.

| | | | |
|---|---|---|---|
| Mo-N1 | 1.963(2) | Mo-O2 | 1.9941(18) |
| Mo-N2 | 1.984(2) | Mo-O3 | 2.0288(18) |
| Mo-O1 | 1.9952(16) | Mo-O4 | 1.9497(16) |
| | | | |
| N1-Mo-N2 | 88.45(9) | N2-Mo-O4 | 84.52(8) |
| N1-Mo-O1 | 74.80(8) | O1-Mo-O2 | 83.70(7) |
| N1-Mo-O2 | 151.42(8) | O1-Mo-O3 | 89.40(7) |
| N1-Mo-O3 | 96.49(8) | O1-Mo-O4 | 165.98(7) |
| N1-Mo-O4 | 109.15(8) | O2-Mo-O3 | 101.97(8) |
| N2-Mo-O1 | 109.25(7) | O2-Mo-O4 | 96.26(7) |
| N2-Mo-O2 | 81.00(8) | O3-Mo-O4 | 76.87(7) |
| N2-Mo-O3 | 161.35(8) | | |

O4 the shortest (1.9497(16) Å). This asymmetry is likely due to the *trans* influence of the amido nitrogen N2, though the $^t$BuClip aryloxides have equivalent Mo–O distances despite O2 being *trans* to amide and O1 being *trans* to catecholate.

There are two possible *cis*-β isomers of the complex. The one that is observed in the solid state (*cis*-β1) has the more electron-rich oxygen of the catecholate (O4, *ortho* and *para* to the *tert*-butyl groups) *trans* to aryloxide. However, DFT calculations (gas-phase, B3LYP) on all three possible geometric isomers of ($^t$BuClip)Mo(3,5-$^t$Bu$_2$Cat) suggest that the two *cis*-β isomers are very similar in energy (Figure 2). The *cis*-α isomer is significantly higher in energy.

The C–C, C–N, and C–O bond lengths of amidophenoxides and catecholates provide useful information about π bonding in their metal complexes, since π donation from these ligands results in a decrease in electron density in the ligand HOMO and characteristic changes in bond distances. These changes parallel those caused by ligand oxidation (which also decreases electron density in the HOMO) and can be quantified by calculating a "metrical oxidation state" (MOS) for each ligand.[17] In ($^t$BuClip)Mo(3,5-$^t$Bu$_2$Cat), amidophenoxide rings containing N1 and N2 show MOS values of –1.44(7) and –1.87(11), respectively, and the catecholate ligand has MOS = –1.85(12). This is consistent with substantial π donation from amidophenoxide ring 1, and weaker π donation from the other two rings. The significant difference between the two amidophenoxide groups is surprising, but it appears to be a genuine electronic effect, as the gas-phase calculation on the *cis*-β1 isomer gives a similar asymmetry (MOS = –1.42(6) and–1.70(10) for the two rings). The overall sum of MOS values, –5.16(13), is similar to the summed MOS values of the seven-coordinate tris(catecholate) complexes Mo$_2$(3,5-$^t$Bu$_2$Cat)$_6$ and (3,5-$^t$Bu$_2$Cat)$_3$Mo(py) (ΣMOS = –5.33(17) and –5.32(15), respectively).[5]

While the bis(amidophenoxide)-monocatecholate complex ($^t$BuClip)Mo(3,5-$^t$Bu$_2$Cat) is isoelectronic with a tris(catecholato)molybdenum complex such as (3,5-$^t$Bu$_2$Cat)$_3$Mo, the latter species has been observed only in seven-coordinate adducts, with the six-coordinate species inferred as a reactive intermediate. The Lewis acidity of the

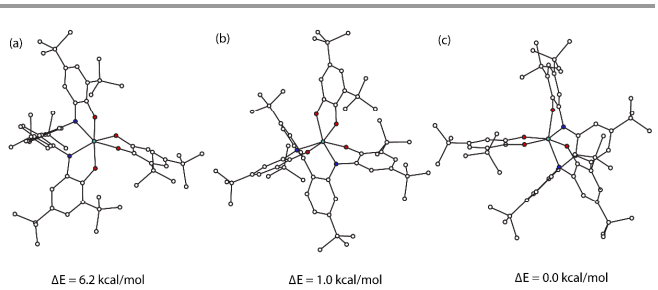


Figure 2. Calculated structures and relative energies (B3LYP, SDD (Mo)/6-31G*) of ($^t$BuClip)Mo(3,5-$^t$Bu$_2$Cat) isomers: (a) *cis*-α, (b) *cis*-β1 and (c) *cis*-β2.

tris(catecholate)molybdenum(VI) fragment has been attributed to the inability of the $A_2$-symmetry ligand π combination to donate to any of the metal $d\pi$ orbitals, which leaves the $d_{z^2}$ orbital low in energy.[5] The lower symmetry of the *cis*-β isomers of ($^t$BuClip)Mo(3,5-$^t$Bu$_2$Cat) removes the symmetry mismatch, allowing some π donation from the amidophenoxides, which stabilizes the orbital and decreases the compound's Lewis acidity. The *cis*-α isomer retains an orbital mismatch, for in $C_2$ symmetry (neglecting the unsymmetrical substitution of the catecholate), the ligand π donor orbitals transform as $A + 2B$, while the metal $d\pi$ orbitals transform as $2A + B$.[18] This may explain its appreciably lower calculated stability compared to the *cis*-β isomers.

**Stereodynamics of ($^t$BuClip)Mo(3,5-$^t$Bu$_2$Cat)**

NMR spectroscopic measurements are consistent with a highly symmetric structure for ($^t$BuClip)Mo(3,5-$^t$Bu$_2$Cat) in solution at room temperature, with seven aromatic resonances and five *tert*-butyl resonances observed in the $^1$H NMR spectrum in $CD_2Cl_2$ (Figure 3a). This apparent symmetry is an artifact of a fluxional process, since each possible isomer is $C_1$-symmetric and should show twelve aromatic and eight *tert*-butyl resonances, as seen at –40 ºC (Figure 3c). Lineshape simulation of the *tert*-butyl region between –30 and +10 ºC gives $\Delta H^{\ddagger}$ = 14.5 ± 0.3 kcal mol$^{-1}$ and $\Delta S^{\ddagger}$ = +8.5 ± 1.3 cal mol$^{-1}$ K$^{-1}$ for the process that exchanges the two halves of the $^t$BuClip ligand in this temperature range. At temperatures below –40 ºC, a number of peaks broaden and shift significantly, but no decoalescence is observed. In particular, the peaks due to the catecholate are affected as much by the temperature changes as the peaks due to the $^t$BuClip ligand, in contrast to their behavior above –40 ºC, where they are sharp. This is suggestive of equilibration between isomers, where the equilibrium position shifts with temperature and the rate slows, but not enough to decoalesce any of the peaks. Thus, ($^t$BuClip)Mo(3,5-$^t$Bu$_2$Cat) likely consists of a mixture of isomers that equilibrate rapidly on the NMR timescale even at -80 ºC.

($^t$BuClip)Mo(3,5-$^t$Bu$_2$Cat) contains two elements of chirality: axial chirality of the 2,2'-disubstituted biphenyl moiety and chirality at the metal center. Combined with the asymmetry of the 3,5-di-*tert*-butylcatecholate, this allows in principle a total of two diastereomers for each of the three

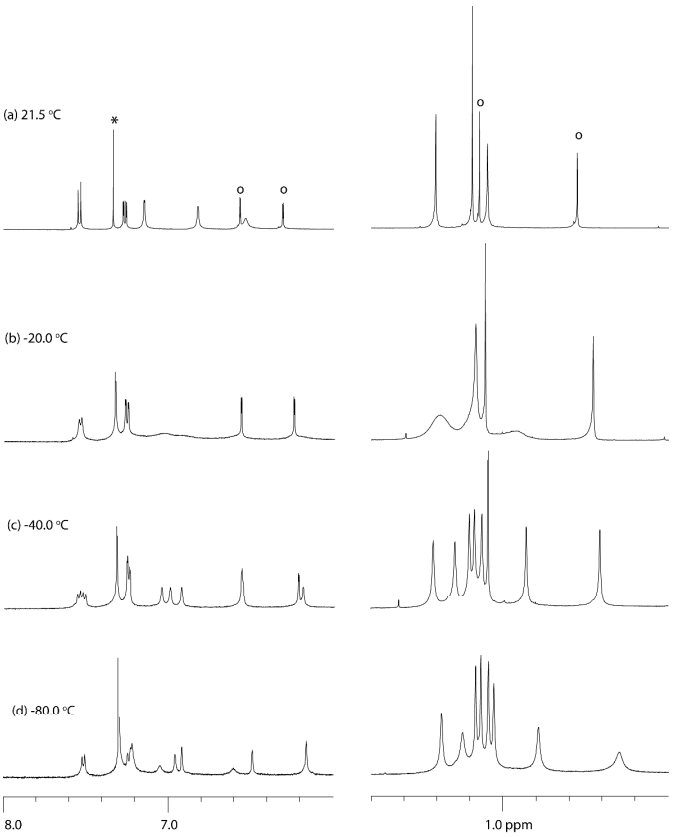


Figure 3. Variable-temperature $^1$H NMR spectra (δ 0.0-1.8 and 6.0-8.0 ppm) of ($^t$BuClip)Mo(3,5-$^t$Bu$_2$Cat) (500 MHz, $CD_2Cl_2$). (a) 21.5 ºC; (b) –20 ºC; (c) –40 ºC; (d) –80 ºC. Peaks due to bound catecholate (o) and $CHCl_3$ (⋆) are marked on the room-temperature spectrum. The vertical scale of the upfield region is reduced relative to the downfield region, but the horizontal scale is the same throughout the spectra.

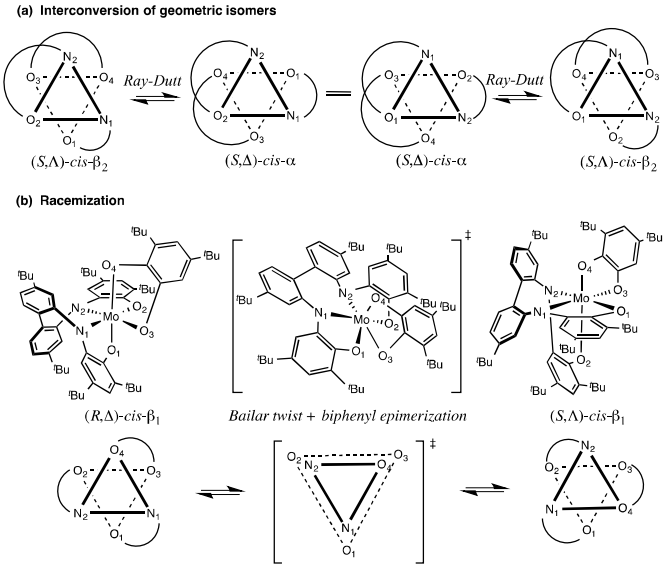


Scheme 1. Stereodynamics of ($^t$BuClip)Mo(3,5-$^t$Bu$_2$Cat). (a) Interconversion of geometric isomers by successive Ray-Dutt twists without epimerization of axial chirality of the biphenyl linker. (b) Racemization by coupled Bailar twist and epimerization of the biphenyl linker.

geometric isomers. However, the physical limitations of the $^t$BuClip ligand in an octahedral tris-chelate environment require that the *cis*-α isomer be the (*S*,Δ)/(*R*,Λ) diastereomer and the *cis*-β isomer the (*S*,Λ)/(*R*,Δ) diastereomer. The alternative diastereomers are not geometrically accessible, in good agreement with the universal observation of these diastereomers in octahedral *cis*-α[19] and cis-β[20] complexes bearing 2,2'-biphenyl- or binaphthyl-bridged bis(salicylaldimine) ligands.

Typically molybdenum catecholate complexes undergo stereoisomerization by trigonal twist mechanisms.[3,21] Since the metal center must undergo inversion of configuration after a trigonal twist, this means that (*S*,Λ)-*cis*-β1 and (*S*,Λ)-*cis*-β2 isomers can interconvert only through the intermediacy of the (*S*,Δ)-*cis*-α isomer via a series of two trigonal (Ray-Dutt) twists (Scheme 1a). These twists are likely to be facile and may explain the changes in the $^1$H NMR spectrum of ($^t$BuClip)Mo(3,5-$^t$Bu$_2$Cat) below –40 ºC, as two (or all three) stereoisomers equilibrate in a temperature-dependent ratio (causing large temperature-dependence of chemical shifts) and at a moderate rate (causing appreciable broadening of some peaks). They cannot, however, explain the symmetrization that takes place in the NMR spectra above –40 ºC, as all three isomers are $C_1$-symmetric and even fast exchange among them would not result in exchange of the chemical environments of the two ends of the $^t$BuClip ligand. In order to explain the high-temperature dynamics, one must invoke racemization, which would require both a trigonal twist (to epimerize at the metal) and twisting about the chiral axis of the biphenyl (to epimerize at the ligand). Since twisting about the biphenyl axis is geometrically precluded if the configuration at the metal is maintained, both twists must occur concurrently. A plausible transition state in such a process is illustrated in Scheme 1b. The observed barrier for this process ($\Delta G^{\ddagger} \approx 12$ kcal mol$^{-1}$) is low, compared to the sum of the barriers for a Bailar twist ($\Delta G^{\ddagger} \approx 9$ kcal mol$^{-1}$ in oxobis(catecholates)[3,21]) and racemization of 2,2'-disubstituted biphenyls (e.g., $\Delta G^{\ddagger} \approx 14$ kcal mol$^{-1}$ for racemization in titanium[18a] and germanium[22] 2,2'-biphenoxides). However, the two events are likely to be strongly coupled. In particular, the N–N distance will likely decrease in the trigonal prism, and the barrier to twisting in 2,2'-disubstituted biphenyls decreases sharply with decreasing equilibrium distance between the substituents. For example, calculated barriers to racemization in boron 2,2'-biphenoxides are ~ 8 kcal mol$^{-1}$.[23] The observed positive $\Delta S^{\ddagger}$ is unexpected, as positive entropies of activation are commonly associated with dissociative mechanisms for racemization. In this case, dissociation of a ligand radical (or anion) is likely to be substantially uphill thermodynamically. It is also difficult to see how ligand dissociation would couple with rotation about the biphenyl axis, which would result in a high overall barrier for this mechanism. While we favor a twist mechanism (Scheme 1b), we do not have a compelling explanation for the positive entropy of activation.

### Preparation and characterization of ($^t$BuClip)Mo(μ-(3,5-$^t$Bu$_2$Cat)$_2$)Mo(O)(3,5-$^t$Bu$_2$Cat)

Addition of excess 3,5-$^t$Bu$_2$CatH$_2$ to ($^t$BuClipH$_2$)MoO$_2$ does not increase the yield of ($^t$BuClip)Mo(3,5-$^t$Bu$_2$Cat). Instead, free $^t$BuClipH$_4$ is formed and a molybdenum-containing byproduct is observed by $^1$H NMR. This byproduct displays a spectrum with sixteen aromatic resonances, consistent with one unsymmetrical $^t$BuClip and three inequivalent di-*tert*-butylcatecholate ligands. Formulation of the product as a dimolybdenum monooxo complex, Mo$_2$(O)($^t$BuClip)(3,5-$^t$Bu$_2$Cat)$_3$, is supported by the observation of a parent ion in its electrospray mass spectrum. The compound is conveniently prepared by self-assembly from dioxomolybdenum bis(acetylacetonate), $^t$BuClipH$_4$ and 3,5-$^t$Bu$_2$CatH$_2$ in a 2:1:3 ratio (eq 2). The dimer is formed in this reaction in nearly quantitative yield, as judged by *in situ* NMR spectroscopy, though isolation is subject to solubility losses. An all-catecholate analogue, Mo$_2$O(3,5-$^t$Bu$_2$Cat)$_5$, was reported in solution as an intermediate in oxygenations of Mo$_2$(3,5-$^t$Bu$_2$Cat)$_6$.[5]

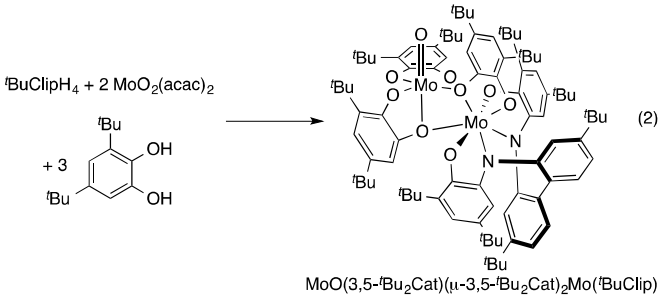


X-ray crystallography (Figure 4) indicates that the compound is an unsymmetrical dimolybdenum complex bridged by two 3,5-di-*tert*-butylcatecholate ligands. One molybdenum, ligated by the $^t$BuClip ligand, adopts an irregular seven-coordinate geometry, while the oxomolybdenum center is octahedral. The structure is a fusion between half of the tris(catecholate) dimer Mo$_2$(3,5-$^t$Bu$_2$Cat)$_6$, and half of the oxobis(catecholate) dimer Mo$_2$O$_2$(3,5-$^t$Bu$_2$Cat)$_4$ (Scheme 2, Table 3).[5,24] The latter compound was previously characterized crystallographically as a toluene solvate in the triclinic space group $P\bar{1}$.[24] We have characterized the same oxomolybdenum dimer as a bis(benzene) solvate in the monoclinic space group $P2_1/c$ (Table 1), where the overall molecular structure and bond distances and angles are essentially the same as in the toluene solvate.

The bridging catecholates in the oxomolybdenum dimer Mo$_2$O$_2$(3,5-$^t$Bu$_2$Cat)$_4$ have an atypical structure in which the plane of the bridging catecholate is strongly inclined with respect to the Mo$_2$O$_2$ diamond core (angle between planes = 55.8° in the toluene solvate,[24] 51.9° in the benzene solvate). The bridging catecholate supplied by the oxomolybdenum fragment in the asymmetric dimer ($^t$BuClip)Mo(μ-(3,5-$^t$Bu$_2$Cat)$_2$)MoO(3,5-$^t$Bu$_2$Cat) likewise makes an angle to the Mo1-O11-Mo2-O21 mean plane of 50.2°. In contrast, the

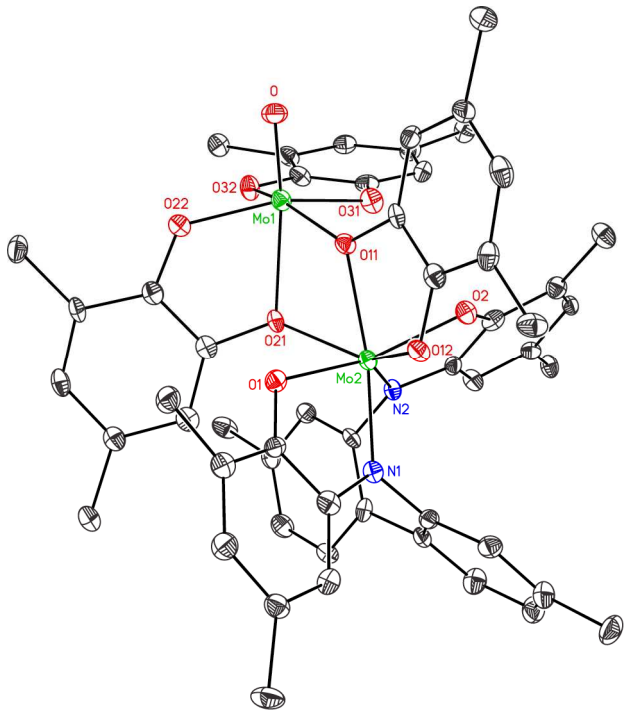


Figure 4. Thermal ellipsoid plot of ($^t$BuClip)Mo(μ-(3,5-$^t$Bu$_2$Cat)$_2$)Mo(O)(3,5-$^t$Bu$_2$Cat)•1.5 C$_6$H$_6$. Solvent molecules, hydrogen atoms and methyl groups are omitted for clarity.

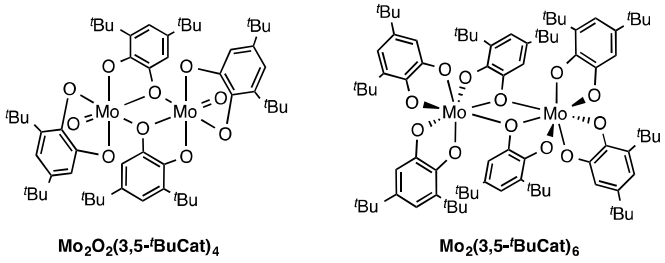


Scheme 2. Dimolybdenum(VI) bis(μ-catecholate) complexes.

bridging catecholate supplied by the seven-coordinate Mo2 center is inclined by only 9.1° to this plane, a nearly coplanar arrangement seen in Mo$_2$(3,5-$^t$Bu$_2$Cat)$_6$ and most other M$_2$(μ-3,5-$^t$Bu$_2$Cat)$_2$ complexes.[5] The catecholates bridge through the less hindered oxygen atoms, and the nonbridging catecholate on Mo1 has its *ortho tert*-butyl group away from the second molybdenum, as observed in Mo$_2$O$_2$(3,5-$^t$BuCat)$_4$. The NMR spectrum of ($^t$BuClip)Mo(μ-(3,5-$^t$Bu$_2$Cat)$_2$)MoO(3,5-$^t$Bu$_2$Cat), which is static and shows only one isomer, strongly suggests that the structure is retained in solution.

The amidophenolate ligands appear to be strongly engaged in π donation to Mo2, as judged from their MOS values (-1.37(7) for the ring containing N1 and –1.39(11) for the ring containing N2). These values are significantly more positive than those observed in the six-coordinate ($^t$BuClip)Mo(3,5-$^t$Bu$_2$Clip), and are close to that observed in the amidophenoxide *trans* to oxo in ($^t$BuClip)MoO(3,5-lutidine) (MOS = -1.34(12)[17]), consistent with π donation of each of the amidophenolates into a *dπ* orbital where there is no competition

**Table 3.** Selected bond distances (Å) in ($^t$BuClip)Mo(μ-(3,5-$^t$Bu$_2$Cat)$_2$)MoO(3,5-$^t$Bu$_2$Cat)•1.5 C$_6$H$_6$ and corresponding distances in Mo$_2$O$_2$(3,5-$^t$Bu$_2$Cat)$_4$•2 C$_6$H$_6$.

| ($^t$BuClip)Mo(μ-(3,5-$^t$Bu$_2$Cat)$_2$)MoO(3,5-$^t$Bu$_2$Cat)•1.5 C$_6$H$_6$ | | Mo$_2$O$_2$(3,5-$^t$Bu$_2$Cat)$_4$•2 C$_6$H$_6$ | |
|---|---|---|---|
| Mo1-O | 1.683(3) | Mo1-O | 1.6844(10) |
| Mo1-O11 | 2.042(2) | Mo1-O3A | 2.0354(9) |
| Mo1-O21 | 2.215(3) | Mo1-O3 | 2.3027(9) |
| Mo1-O22 | 1.930(3) | Mo1-O4 | 1.9233(9) |
| Mo1-O31 | 1.948(3) | Mo1-O1 | 1.9400(9) |
| Mo1-O32 | 1.954(3) | Mo1-O2 | 1.9476(9) |
| Mo2-N1 | 2.015(3) | | |
| Mo2-N2 | 2.039(3) | | |
| Mo2-O1 | 2.008(3) | | |
| Mo2-O2 | 2.027(3) | | |
| Mo2-O11 | 2.159(2) | | |
| Mo2-O12 | 1.987(3) | | |
| Mo2-O21 | 2.146(2) | | |

from other π-donor ligands. The apparently weaker π donation in the six-coordinate complex may be due to competition from the catecholate (bridging catecholates are generally poor π donors).

### Pyridine binding to ($^t$BuClip)Mo(3,5-$^t$Bu$_2$Cat)

In contrast to Mo(3,5-$^t$Bu$_2$Cat)$_3$, the bis(amidophenolate)-catecholate complex ($^t$BuClip)Mo(3,5-$^t$Bu$_2$Cat) is isolable as a six-coordinate monomer. Nevertheless, the facile formation of a seven-coordinate ($^t$BuClip)Mo complex in dimetallic ($^t$BuClip)Mo(μ-(3,5-$^t$Bu$_2$Cat)$_2$)MoO(3,5-$^t$Bu$_2$Cat) is evidence that ($^t$BuClip)Mo(3,5-$^t$Bu$_2$Cat) retains some Lewis acidity.

Further evidence of the Lewis acidity of ($^t$BuClip)Mo(3,5-$^t$Bu$_2$Cat) is provided by its reaction with pyridine to form a seven-coordinate adduct (eq 3). The $^1$H NMR spectrum of the adduct in $CD_2Cl_2$ (Figure 5) shows peaks that are broad at ambient temperature, but sharp at temperatures below –20 ºC. Integration of the signals due to bound pyridine is consistent with binding of one pyridine per molybdenum center.

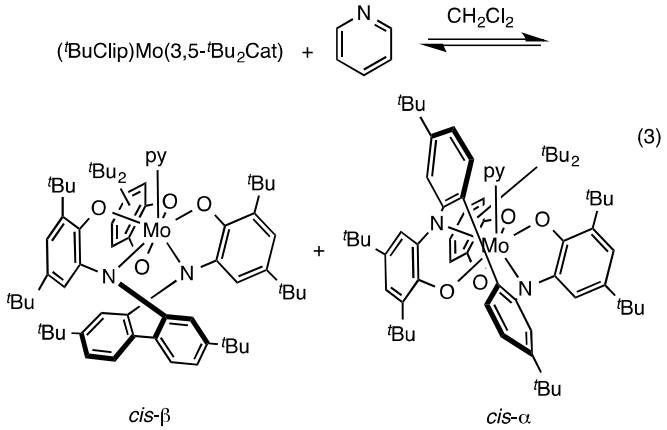


(3)

The tris(catecholate) analogue, (3,5-$^t$Bu$_2$Cat)$_3$Mo(py), adopts a capped octahedral structure of approximate $C_3$ symmetry (neglecting the *tert*-butyl groups).[5] Presumably ($^t$BuClip)Mo(3,5-$^t$Bu$_2$Cat)(py) adopts an analogous structure, with catecholate and two amidophenoxides spanning the capped and uncapped octahedral faces. The two nitrogen atoms of the $^t$BuClip ligand would likely avoid occupying positions on the capped face, since that face is substantially expanded to

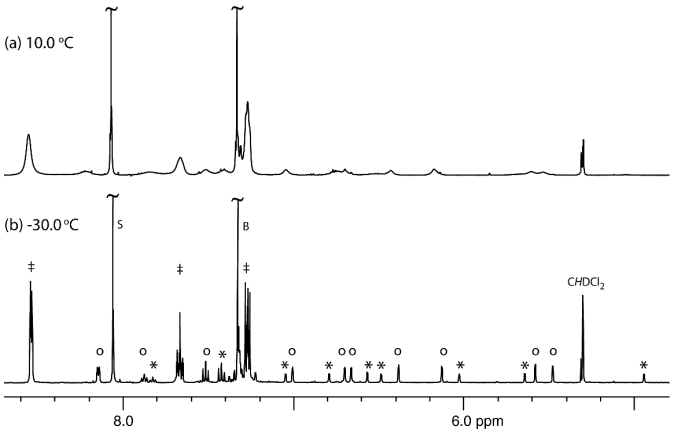


Figure 5. Partial $^1$H NMR spectra (δ 4.8-8.7 ppm, 500 MHz, $CD_2Cl_2$) of ($^t$Bu$_2$Clip)Mo(3,5-$^t$Bu$_2$Cat) in the presence of pyridine at (a) 10 ºC and (b) –30 ºC. Key: Major isomer(s) of ($^t$Bu$_2$Clip)Mo(3,5-$^t$Bu$_2$Cat)(py) (o), minor isomer(s) (*), free pyridine (‡), benzene (B), and dimethyl terephthalate (S, added as an internal standard).

accommodate the pyridine ligand (O-Mo-O = 112(4)º in (3,5-$^t$Bu$_2$Cat)$_3$Mo(py)[5]), and the N-Mo-N angle in known ($^t$BuClip)Mo complexes is always less than 90º (81.8–88.4º in six-coordinate metal centers,[7] and 82.58(12)º in seven-coordinate Mo$_2$(O)($^t$BuClip)(3,5-$^t$Bu$_2$Cat)$_3$). The 2,2'-biphenyl group could bridge between two nitrogen atoms in the face opposite the capping pyridine (*cis*-β) or between this face and the capped face (*cis*-α). The geometrical constraints of these two arrangements are similar in (3,5-$^t$Bu$_2$Cat)$_3$Mo(py) (O-Mo-O = 82.16(12)º and 82.7(22)º, respectively).[5] The *cis*-α and *cis*-β geometries would each have two isomers, depending on the orientation of the *tert*-butyl groups of the 3,5-$^t$Bu$_2$Cat ligand.

The $^1$H NMR spectrum of ($^t$BuClip)Mo(3,5-$^t$BuClip)(py) at low temperature (Figure 5b) displays two sets of signals in unequal amounts (e.g., a 2.3:1 ratio at –30 ºC). Each set consists of resonances due to an unsymmetrical $^t$BuClip ligand, one catecholate ligand, and one pyridine. It is possible that each of these sets of signals represents a single isomer, but more likely that each set of signals represents a rapidly equilibrating pair of isomers. For example, the two *cis*-α isomers could be rapidly equilibrating with each other, but only slowly interconverting with the two *cis*-β isomers. The presence of multiple isomers interconverting rapidly is precedented in (3,5-$^t$Bu$_2$Cat)$_3$Mo(py), which shows only a single catecholate environment by $^1$H NMR even at –70 ºC despite the crystallization of the compound as the unsymmetrical isomer.[5] An unusually high temperature-dependence of the chemical shifts of the resonances in ($^t$BuClip)Mo(3,5-$^t$BuClip)(py) is also suggestive of the presence of a fast (temperature-dependent) equilibration of isomers within each discrete set of signals.

At higher temperatures, $^1$H NMR spectra of ($^t$BuClip)Mo(3,5-$^t$BuClip)(py) indicate that free and bound pyridine are exchanging on the NMR timescale (Figure 5a). Since the linewidth of the resonances due to bound pyridine are independent of the concentration of free pyridine in the slow



 

exchange regime, this indicates that the exchange mechanism is dissociative, as expected for a seven-coordinate adduct. Quantitative lineshape simulation of the bound and free pyridine resonances at 0 ºC gives similar dissociation rate constants for the pyridines associated with the major and minor sets of isomers ($k_{diss}$ = 25 ± 3 $s^{-1}$, $\Delta G^{\ddagger}_{diss}$ = 14.2 kcal $mol^{-1}$). While dissociation of pyridine also results in exchange between isomers, we cannot exclude an additional intramolecular pathway for exchange of isomers. This complication prevents successful simulation of the spectra in the fast-exchange regime, and we were therefore unable to determine activation parameters for the exchange.

Pyridine binding can also be observed by UV-visible spectroscopy. Titration of solutions of ($^t$BuClip)Mo(3,5-$^t$Bu$_2$Cat) in $CH_2Cl_2$ with pyridine under anaerobic conditions results in a colour change from dull to vibrant purple with corresponding changes in the optical spectrum (Figure 6). In particular, the three features in the visible spectrum of ($^t$BuClip)Mo(3,5-$^t$Bu$_2$Cat) at $\lambda_{max}$ = 743 nm (ε = 5400 L $mol^{-1}$ $cm^{-1}$), 496 nm (18000 L $mol^{-1}$ $cm^{-1}$) and 403 nm (11000 L $mol^{-1}$ $cm^{-1}$) shift on addition of pyridine to longer wavelengths ($\lambda_{max}$ = 767 nm, 550 nm and a shoulder at 450 nm). Analysis of the spectra as a function of added pyridine allow calculation of the binding constant of pyridine, and its variation from 284-308 K gives thermodynamic parameters for binding of $\Delta H^{o}$ = –10.9 ± 0.7 kcal $mol^{-1}$ and $\Delta S^{o}$ = –23.9 ± 2.4 cal $mol^{-1}$ $K^{-1}$ (Figure 6, inset).

($^t$Bu$_2$Clip)Mo(3,5-$^t$Bu$_2$Cat) is unique compared to its analogues ($^t$BuClip)MoO and (3,5-$^t$Bu$_2$Cat)$_3$Mo in that only the mixed amidophenoxide-catecholate can be observed as a stable monomeric compound. This indicates that the mixed amidophenoxide-catecholate compound is the least Lewis acidic. This is chemically reasonable, since it has both a high coordination number (making ligand binding less favorable than in the oxo complex), and has more electron-donating ligands (amidophenolate vs. catecholate). The fragment with both amidophenolate → catecholate and catecholate → oxo substitutions, (3,5-$^t$Bu$_2$Cat)$_2$MoO, is markedly more Lewis acidic, as judged by the observation that pyridine substitution in (3,5-$^t$Bu$_2$Cat)$_2$MoO(py) is both much slower than in any of the other three adducts and takes place by an associative, not dissociative, mechanism.[3]

Surprisingly, the qualitatively lower Lewis acidity of the mixed amidophenolate-catecholate complex is not apparent in the dissociation rate of pyridine from ($^t$BuClip)Mo(3,5-$^t$Bu$_2$Cat)(py). Dissociation of pyridine from ($^t$BuClip)Mo(3,5-$^t$Bu$_2$Cat)(py) at 0 ºC ($\Delta G^{\ddagger}_{273K}$ = 14.2 kcal $mol^{-1}$) is intermediate in rate between ($^t$BuClip)MoO(py) ($\Delta G^{\ddagger}_{273K}$ = 14.7 kcal $mol^{-1}$)[7] and (3,5-$^t$Bu$_2$Cat)$_3$Mo(py) ($\Delta G^{\ddagger}_{273K}$ = 13.6 kcal $mol^{-1}$),[5] and the overall span of rates among the three is only about a factor of 10 between fastest and slowest. Extrapolating the equilibrium binding data for ($^t$BuClip)Mo(3,5-$^t$Bu$_2$Cat)(py) using the van't Hoff plot gives $\Delta G^{o}_{binding,\ 273K}$ = –4.4 kcal $mol^{-1}$ and thus $\Delta G^{\ddagger}_{binding,\ 273K}$ = 9.8 kcal $mol^{-1}$ ($k_{assoc}$ = 8 × $10^4$ L $mol^{-1}$ $s^{-1}$, eq 4).

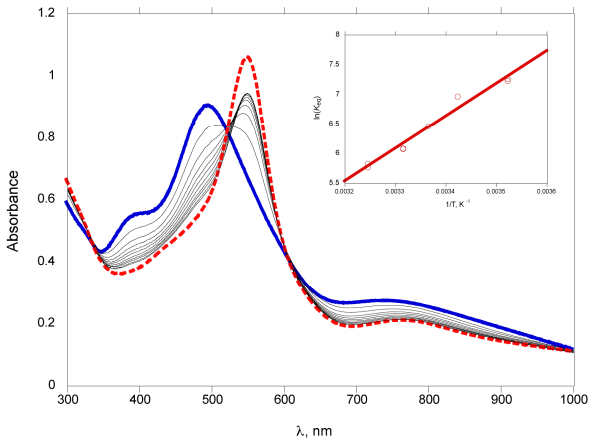


Figure 6. UV-visible titration of ($^t$Bu$_2$Clip)Mo(3,5-$^t$Bu$_2$Cat) (5 × $10^{-5}$ mol $L^{-1}$) with pyridine ($CH_2Cl_2$, 24 ºC). The thick solid line is the initial spectrum of ($^t$Bu$_2$Clip)Mo(3,5-$^t$Bu$_2$Cat) and the thick dashed line is the final (calculated) spectrum of ($^t$Bu$_2$Clip)Mo(3,5-$^t$Bu$_2$Cat)(py). Thin solid lines correspond to successive additions of pyridine to give concentration increments of 6.2 × $10^{-4}$ mol $L^{-1}$. Inset: van't Hoff plot of $K_{eq}$ for binding, 284–308 K.

($^t$BuClip)Mo(3,5-$^t$Bu$_2$Cat) + py ⇌ ($^t$BuClip)Mo(3,5-$^t$Bu$_2$Cat)(py) (4)
$k_{assoc}$ = 8 x $10^4$ L $mol^{-1}$ $s^{-1}$
$k_{diss}$ = 25 $s^{-1}$
$T$ = 273 K

In typical dissociative ligand substitution reactions of six-coordinate complexes, ligand (re)binding to the five-coordinate intermediate is usually very fast.[25] Chemists are thus accustomed to attributing the differences in *kinetic* parameters of dissociative ligand substitution nearly entirely to differences in *thermodynamics* of ligand binding (since $\Delta G^{\ddagger}_{rebinding} \approx 0$).[26] In ligand exchange reactions of ($^t$BuClip)MoO(py), there is stereochemical evidence consistent with a short lifetime for the five-coordinate intermediate, in that stereoisomers of the product do not interconvert during dissociation/reassociation of pyridine.[7] The comparatively slow binding kinetics of pyridine to the six-coordinate ($^t$BuClip)Mo(3,5-$^t$Bu$_2$Cat) suggests that this usual assumption may not be valid for dissociative reactions of *seven*-coordinate species. It is clear that the apparently lower Lewis acidity of ($^t$BuClip)Mo(3,5-$^t$Bu$_2$Cat) compared to (3,5-$^t$Bu$_2$Cat)$_3$Mo or ($^t$BuClip)MoO is not reflected in the very similar rates of ligand dissociation. Perhaps in this case, differences in the ligand coordination rates to the unsaturated species are more sensitive to the metal structure and bonding, and thus the lower thermodynamic affinity of ($^t$BuClip)Mo(3,5-$^t$Bu$_2$Cat) for pyridine is expressed principally in its low rate of binding rather than in high rates of dissociation of ($^t$BuClip)Mo(3,5-$^t$Bu$_2$Cat)(py).

## Conclusions

Mixed amidophenolate-catecholate complexes of molybdenum(VI) are prepared by treatment of the bis(aminophenoxide) complex ($^t$BuClipH$_2$)MoO$_2$ with 3,5-di-*tert*-butylcatechol. The bis(amidophenoxide)-monocatecholate complex ($^t$BuClip)Mo(3,5-$^t$Bu$_2$Cat) is stable as a monomeric, distorted octahedral complex. In the solid state, one *cis*-β

isomer is observed, but solution NMR data and DFT calculations are consistent with facile interconversion between this isomer and the other *cis*-β isomer via the *cis*-α isomer. Racemization of the complex, necessarily involving atropisomerization of the 2,2'-biphenylene bridge, is also observed by NMR. Use of excess catechol results in production of an asymmetric catecholate-bridged dimer. Six-coordinate ($^t$BuClip)Mo(3,5-$^t$Bu$_2$Cat) is appreciably Lewis acidic, with pyridine binding ($K_{binding}$ = 640 L mol$^{-1}$ at 24 ºC) apparent both by UV-visible and NMR spectroscopy. In contrast to its analogues with catecholates in place of amidophenolates ([3,5-$^t$Bu$_2$Cat]$_3$Mo) or oxo in place of catecholate ([$^t$BuClip]MoO), the mixed amidophenolate-catecholate can be observed as a stable compound, indicating that it has reduced Lewis acidity compared to these analogues. This is consistent with amidophenolate's greater electron donating ability relative to catecholate and catecholate's greater steric profile relative to oxo. This lower Lewis acidity is not reflected kinetically in the dissociation rate of pyridine, which is similar in all three pyridine adducts. Instead, it manifests itself principally in the low rate of binding of pyridine to ($^t$BuClip)Mo(3,5-$^t$Bu$_2$Cat) ($k_{273K}$ = 8 × 10$^4$ L mol$^{-1}$ s$^{-1}$).

## Acknowledgements

This work was generously supported by a grant from the US National Science Foundation (CHE-1112356). We thank Dr. Allen G. Oliver for his assistance with the X-ray crystallography.

## Notes and references

[a]*Department of Chemistry and Biochemistry, 251 Nieuwland Science Hall, University of Notre Dame, Notre Dame, IN 46556-5670, USA. Fax: 01 574 631 6652; Tel: 01 574 631 4659; E-mail: Seth.N.Brown.114@nd.edu*

Electronic Supplementary Information (ESI) available: Energies and Cartesian coordinates for calculated structures of isomers of ($^t$BuClip)Mo(3,5-$^t$Bu$_2$Cat). Crystallographic data in CIF format have been deposited with the CCDC, deposition numbers 976190-976192. See DOI: 10.1039/b000000x/

1 (a) C. G. Pierpont and C. W. Lange, *Prog. Inorg. Chem.*, 1994, **41**, 331-442. (b) C. G. Pierpont, *Coord. Chem. Rev.*, 2001, **219-221**, 415-433.
2 R. F. Munhá, R. A. Zarkesh and A. F. Heyduk, *Dalton Trans.*, 2013, **42**, 3751-3766.
3 T. Marshall-Roth, S. C. Liebscher, K. Rickert, N. J. Seewald, A. G. Oliver and S. N. Brown, *Chem. Commun.*, 2012, **48**, 7826-7828.
4 M. E. Cass and C. G. Pierpont, *Inorg. Chem.*, 1986, **25**, 122-123.
5 A. H. Randolph, N. J. Seewald, K. Rickert and S. N. Brown, *Inorg. Chem.*, 2013, **52**, 12587-12598.
6 (a) K. J. Blackmore, J. W. Ziller and A. F. Heyduk, *Inorg. Chem.*, 2005, **44**, 5559-5561. (b) K. J. Blackmore, M. B. Sly, M. R. Haneline, J. W. Ziller and A. F. Heyduk, *Inorg. Chem.*, 2008, **47**, 10522-10532.
7 J. A. Kopec, S. Shekar and S. N. Brown, *Inorg. Chem.*, 2012, **51**, 1239-1250.
8 P. H. M. Budzelaar, *gNMR*, v. 3.5.6, Cherwell Scientific Publishing, 1996.
9 W. H. Lawton and E. A. Sylvestre, *Technometrics*, 1971, **13**, 461-467.
10 D. C. Harris, *J. Chem. Educ.*, 1998, **75**, 119-121.
11 M. J. Frisch, G. W. Trucks, H. B. Schlegel, G. E. Scuseria, M. A. Robb, J. R. Cheeseman, G. Scalmani, V. Barone, B. Mennucci, G. A. Petersson, H. Nakatsuji, M. Caricato, X. Li, H. P. Hratchian, A. F. Izmaylov, J. Bloino, G. Zheng, J. L. Sonnenberg, M. Hada, M. Ehara, K. Toyota, R. Fukuda, J. Hasegawa, M. Ishida, T. Nakajima, Y. Honda, O. Kitao, H. Nakai, T. Vreven, J. A. Montgomery, Jr., J. E. Peralta, F. Ogliaro, M. Bearpark, J. J. Heyd, E. Brothers, K. N. Kudin, V. N. Staroverov, R. Kobayashi, J. Normand, K. Raghavachari, A. Rendell, J. C. Burant, S. S. Iyengar, J. Tomasi, M. Cossi, N. Rega, J. M. Millam, M. Klene, J. E. Knox, J. B. Cross, V. Bakken, C. Adamo, J. Jaramillo, R. Gomperts, R. E. Stratmann, O. Yazyev, A. J. Austin, R. Cammi, C. Pomelli, J. W. Ochterski, R. L. Martin, K. Morokuma, V. G. Zakrzewski, G. A. Voth, P. Salvador, J. J. Dannenberg, S. Dapprich, A. D. Daniels, O. Farkas, J. B. Foresman, J. V. Ortiz, J. Cioslowski and D. J. Fox, *Gaussian 09, Revision A.02*, Gaussian, Inc., Wallingford CT, 2009.
12 A. L. Spek, *Acta Cryst. D*, 2009, **D65**, 148-155.
13 G. M. Sheldrick, *Acta Cryst. A*, 2008, **A64**, 112-122.
14 *International Tables for Crystallography*; Kluwer Academic Publishers: Dordrecht, The Netherlands, 1992, Vol C.
15 C. Mukherjee, T. Weyhermüller, E. Bothe and P. Chaudhuri, *Inorg. Chem.*, 2008, **47**, 11620-11632.
16 P. D. Knight and P. Scott, *Coord. Chem. Rev.*, 2003, **242**, 125-143.
17 S. N. Brown, *Inorg. Chem.*, 2012, **51**, 1251-1260.
18 (a) N. Kongprakaiwoot, M. Quiroz-Guzman, A. G. Oliver and S. N. Brown, *Chem. Sci.*, 2011, **2**, 331-336. (b) S. N. Brown, E. T. Chu, M. W. Hull and S. N. Brown, *J. Am. Chem. Soc.*, 2005, **127**, 16010-16011.
19 (a) P. R. Woodman, I. J. Munslow, P. B. Hitchcock and P. Scott, *J. Chem. Soc., Dalton Trans.*, 1999, 4069-4076. (b) P. R. Woodman, N. W. Alcock, I. J. Munslow, C. J. Sanders and P. Scott, *J. Chem. Soc., Dalton Trans.*, 2000, 3340-3346. (c) P. D. Knight, P. N. O'Shaughnessy, I. J. Munslow, B. S. Kimberley and P. Scott, *J. Organomet. Chem.*, 2003, **683**, 103-113. (d) P. N. O'Shaughnessy, P. D. Knight, C. Morton, K. M. Gillespie and P. Scott, *Chem. Commun.*, 2003, 1770-1771. (e) P. D. Knight, G. Clarkson, M. L. Hammond, B. S. Kimberley and P. Scott, *J. Organomet. Chem.*, 2005, **690**, 5125-5144. (f) F. Zhang, H. Song and G. Zi, *Dalton Trans.*, 2011, **40**, 1547-1566.
20 (a) M.-C. Cheng, M. C.-W. Chan, S.-M. Peng, K.-K. Cheung and C.-M. Che, *J. Chem. Soc., Dalton Trans.*, 3479-3482. (b) X.-G. Zhou, J.-S. Huang, P.-H. Ko, K.-K. Cheung and C.-M. Che, *J. Chem. Soc., Dalton Trans.*, 1999, 3303-3309. (c) P. R. Woodman, C. J. Sanders, N. W. Alcock, P. B. Hitchcock and P. Scott, *New J. Chem.*, 1999, **23**, 815-817. (d) I. J. Munslow, K. M. Gillespie, R. J. Deeth and P. Scott, *Chem. Commun.*, 2001, 1638-1639. (e) D. A. Evans, J. M. Janey, N. Magomedov and J. S. Tedrow, *Angew. Chem. Int. Ed.*, 2001, **40**, 1884-1888. (f) R. A. Coxall, L. F. Lindoy, H. A. Miller, A. Parkin, S. Parsons, P. A. Tasker and D. J. White, *Dalton Trans.*, 2003, 55-64. (g) M. Shi and W.-L. Duan, *Appl. Organomet. Chem.*, 2003, **17**, 175-180. (h) A. Soriente, M. De Rosa, M. Lamberti, C. Tedesco, A. Scettri and C. Pellecchia, *J. Mol. Catal. A: Chem.*, 2005, **235**, 253-259. (i) M. Strianese, M. Lamberti, M. Mazzeo, C. Tedesco and C. Pellecchia, *J. Mol. Catal. A: Chem.*, 2006, **258**, 284-291. (j) B. Saha, M.-H. Lin and T. V. RajanBabu, *J. Org. Chem.*, 2007, **72**, 8648-8655. (k) Z.-J. Xu, R. Fang, C. Zhao, J.-S. Huang, G.-Y. Li, N. Zhu and C.-M. Che, *J. Am. Chem. Soc.*, 2009, **131**, 4405-4417. (l) L. Clowes, M. Walton, C. Redshaw, Y. Chao, A. Walton, P. Elo, V. Sumerin and D. L. Hughes, *Cat. Sci. Tech.*, 2013, **3**, 152-160.
21 C.-M. Liu, E. Nordlander, D. Schmeh, R. Shoemaker and C. G. Pierpont, *Inorg. Chem.*, 2004, **43**, 2114-2124.
22 S. D. Pastor, A. Carinci, N. Khoury and D. N. Rahni, *Inorg. Chem.*, 2001, **40**, 3830-3832.
23 J. A. Raskatov, J. M. Brown and A. L. Thompson, *CrystEngComm*, 2011, **13**, 2923-2929.
24 R. M. Buchanan and C. G. Pierpont, *Inorg. Chem.*, 1979, **18**, 1616-1620.
25 (a) R. Bonneau and J. M. Kelly, *J. Am. Chem. Soc.*, 1980, **102**, 1220-1221. (b) M. J. Gaudin, C. R. Clark and D. A. Buckingham, *Inorg. Chem.*, 1986, **25**, 2569-2575. (c) J. E. Shanoski, C. K. Payne, M. F. Kling, E. A. Glascoe and C. B. Harris, *Organometallics*, 2005, **24**, 1852-1859.
26 R. R. Conry and J. M. Mayer, *Inorg. Chem.*, 1990, **29**, 4862-4867.



 